NUMERICAL MODELING OF FRACTURE IN CONCRETE USING FRACTAL THEORY AND COMPARISON WITH AE BASED *b* - VALUE

R.Vidya Sagar*, B.K.Raghu Prasad**

Department of Civil Engineering, Indian Institute of Science, Bangalore,560012, India

***Advisor, Indian Institute of Science, Bangalore 560012, India*

Summary Singular fractal functions (SFF) were used to generate stress-strain plots for quasi-brittle material like concrete and cement mortar and subsequently stress-strain plot of cement mortar was used for numerical modelling of fracture process in concrete. Lattice model was used to study concrete fracture by considering softening of matrix (cement mortar). The results obtained from simulations show softening behavior of concrete and fairly agree with the experimental results. The number of fractured elements were compared with the acoustic emission (AE) hits. The trend in the cumulative fractured beam elements in the lattice fracture simulation reasonably reflected the trend in the recorded AE measurements and variation in AE based b-value. In other words, the pattern in which AE hits were distributed around the notch in the three point bend specimen has the same trend as that of the fractured elements around the notch which is in support of lattice model.

INTRODUCTION

Researchers considered fracture surfaces and crack patterns of quasi-brittle materials like concrete as fractals. Fractal is a shape made of parts similar to the whole in some way [1]. Fracture surfaces of the quasi-brittle materials and also crack patterns are considered as irregular objects called natural fractals [1-3]. The idea to distribute fractures in a plate as a Cantor dust is introduced by Mosolov and later genarilzed the idea of Bernstein et al. and suggested to describe not completely smooth processes using SFF [4]. At the microscale level the damage in the material is the accumulation of microstresses in the neighborhood of defects or interfaces and the breaking of bonds [4]. Both accumulation of micro cracks and breaking of bonds cause damage to the material. It is necessary to consider the fractal nature of crack when simulating fracture process in quasi-brittle materials like concrete. However, repeated observation at various magnifications also reveals a variety of additional structures that fall between the 'micro' and the 'macro' and have not yet been described satisfactorily in a systematic manner. In fact researchers studied that fractal dimension is a measure of toughness in metals and concrete and concluded that tougher the material, higher the fractal dimension. By following Mosolov, in the present study a 2D lattice model for simulating fracture is used in which softening of matrix (cement mortar) is implemented[3-4]. In the authors opinion a comparison of fractured lattice elements with AE measurements would be of major interest because it would allow to better understand the capability of the lattice model in predicting the formation of micro-cracks, both in the pre-peak and in the post-peak regime. An attempt has been made to compare the fractured elements in the lattice network with the AE based b-value. A Cantor set is characterized by describing its generation as a single line of unit length(initiator). Suppose a bar of unit length and assume that it's is density $\rho_0 =1$. The original bar has a length l_0 and therefore the mass $p_0=1$. The operation of applying generator now consists of cutting the bar into two halves of equal mass $p_1=p_2=0.5$, and then hammering the two halves so that the length of each part of the bar becomes $l_1=1/3$. By this process the density increases to $\rho_1 = p_1/l_1 = 3/2$. Repeating this process, the n^{th} generation will be $N=2^n$ small bars, each with a length $l_i=3^{-n}$ and a mass $p_i=2^{-n}$ for i=1,2,3………….N. Note that the process conserves the mass so that

$$\sum_{i=1}^{N} p_i = 1 \qquad (1)$$

This process is known as curdling since an originally uniform mass distributed by this process clumps(or bundled) together into many small regions with a high density [1]. The mass restricted in the segment [0,x] of the interval [0,1] can be written as cm(x).

$$cm(x) = \int_0^x p(\beta)d\beta \qquad (2)$$

The plot between the cm(x) versus x is known as devil's staircase. From Fig.2 it can be observed that the function cm(x) is almost horizontal and its derivation is almost everywhere zero.

$$\frac{d}{dx}[cm(x)] \cong 0 \qquad (3)$$

It has been well cited in the literature that damage is deterioration of the material before leading to debonding from the level of atoms to the mesoscale level [4]. By using the concepts from damage mechanics, the evolution of damage can be represented by a parameter η, called damage parameter [3]. Following Mosolov, Youngs's modulus could be considered to be decreasing as damage progress and then it becomes a function of η[4]. Let the strain energy density function for an elastic material, U(ε,η) is defined as

$$U = \frac{E(\eta)\varepsilon^2}{2} \qquad (4)$$

$E(\eta)$ is an elastic modulus, ε is strain, η is a damage parameter ($0 \le \eta \le 1$).

Further, expressing η as a function of strain, ε [4]

$$E(\eta) = E_0[1-\eta(\varepsilon)] \qquad (5)$$

Further damage is a function of strain ε, because idealizing stress-strain particularly in the post-peak region as S.F.F due to reasons mentioned earlier, one can say that $\frac{d\eta(\varepsilon)}{d\varepsilon} \cong 0$ everywhere although the stress-strain plot is continuous, which is a typical feature of S.F.F [1,4].

Substituting eq.(5) into $\sigma = E\varepsilon$

$$\sigma = E[\varepsilon - \eta(\varepsilon)\varepsilon] \qquad (5)$$

For apparent (noticeable) strain equal to ε, if the fraction of ε, which has been released by the structure made of a quasi-brittle material like concrete, is equal to η (ε), then the stress-strain relation becomes as given in eq. (5). Using the eq. (5) stress-strain plot for a quasi brittle material is generated by replacing $\eta(\varepsilon)$ by cm(x) and ε by cumulative length (x). The lattice beam elements belongs to cement mortar are assumed to follow a strain softening law[Fig.1]. Here the stress strain law for cement mortar was generated using SFF and the limiting strains (ε_{cr}, ε_{cru}) are assumed only in case of cement mortar from generated SFF plot as shown in Fig.1. The failure criterion in case of lattice elements belongs to cement mortar after reaching the peak stress is followed using eq.(21).

$$\sigma = \sigma_t - \frac{(\varepsilon - \varepsilon_{cr})}{(\varepsilon_{cru} - \varepsilon_{cr})} * \sigma_t \qquad (6)$$

σ= current stress ,σ_t= stress at peak load (peak stress),ε_{cr} = initial cracking strain (strain at peak stress),ε = current strain ε_{cru} = failure strain

2. Results and discussion

Notched beams of depth 80mm with a constant span to depth ratio of 3, thickness 80mm and span 240mm were tested in three-point bending. The notch to depth ratios were selected to be 0.15. The specimens were tested under crack mouth opening displacement (CMOD) control at a constant rate of 0.0004 mm/sec. Concrete mix (78 MPa) with coarse aggregate of maximum size 20mm was used. The AE system used had 8 channels (PAC 2005). The sensors R6D are resonant type differential AE transducers with the highest sensitivity at 50 kHz frequency. AE signals of amplitude over 40 dB were recorded along with the associated signal parameters. The mid-span displacement was measured using a linearly varying displacement transformer (LVDT). In the present study singular fractal functions are used to generate stress – strain plots for different values of p &λ. As p (mass) increases the peak stress decreases. The authors opinion is as the crack progresses in the uncracked ligament it could be considered as the line x, getting divided into smaller parts similar to the explanation given in cantor and curdling section. The strain energy stored is proportional to the volume and therefore the mass of the beam. As the uncracked ligament (D-a_0) becomes smaller and smaller, the strain energy has to be transmitted across smaller ligaments. This could be considered as exactly similar to what is happening when the mass p is distributed on the divided lines x as earlier demonstrated in the section Cantor set and curdling. In the present study, the mass p and the line x are divided in such a way that larger p is made to act on a smaller line ligament while in the later case it is similar to where p & x are divided in the same proportion. Mosolov [4] showed that for different combinations of p & λ, it is possible to obtain different types of stress-deformation plots from eq.(6). Generally, it can be seen that larger values of λ with smaller p give a linear prepeak and almost brittle post peak responses, while smaller λ & larger p show a linear pre-peak but a softening type of post peak. Therefore several smaller λ & larger p combinations are tried to obtain a very near actual stress–deformation behaviour of plain concrete in tension as shown in Fig.1. Evans and Marathe [5] studied microcracking in concrete under tension and obtained stress-strain curves for different concrete mixes. Fig.2 show the plots related to stress-strain behaviour under tension for concrete with progressive damage obtained using SFF approach along with experimental results by Evans and Marathe [5] and it is observed that there is similarity between them to some extent and hence it has validated the applicability of SFF for representation of constitutive law for concrete as shown in Fig.2. However, as the stress deformation plots of concrete are strongly specimen size dependent it requires different combinations of λ and p, which provide a close relationship with experimental results before one can generalize. As p increases the peak stress decreases and also the softening slope increases, In other words it is tending to brittle failure. The fracture process during tension near the notch very closely represents the curdling process. It could be called the cascading type of failure. As fracture process proceeds more debonding occurs between the aggregates [1-4]. It can be said that the energy release rate which is obviously nonlinear in concrete could be considered very close to singular fractal functions. A typical plot of load versus CMOD recorded during the experiment is shown in Fig.2. It is interesting to note that CMOD obtained from the lattice model analysis agrees fairly well with the experimental results. It was observed from the analysis that the bond elements were the first to fail under increased loading and that the number of fractured elements increased near, and after, the peak load, i.e. once the crack starts to propagate. The specific fracture energy of the concrete used in this study determined according to the RILEM Committee 50-FMC recommendations (RILEM 1985[5]) is 180.6 N/m. After the peak-load, both the AE energy released and the number of fractured lattice elements is increased. Table 1 shows the load, time, number of AE hits occurring during the fracture of the TPB specimen, and the number of fractured lattice elements. Most of the AE activity takes place on either side of the pre-existing notch tip, thus justifying the use of the lattice network model only in the middle third of the beam. The trend in the cumulative number of recorded AE events with load, as shown in the Table 1 matches closely the trend in the cumulative number of fractured elements. It is interesting to see that the sequence and quantum of fractured members of the lattice matches moderately with the trend of the occurrence of AE events. The most likely causes behind the mismatch between number of fractured lattice elements and the AE parameters are the following. (a) Attenuation of the ultrasonic waves between the source and sensor due to wave scatter and internal damping. (b) Scattering of acoustic waves by the heterogeneities present in the concrete mix particularly by the interfaces (c) The length of the lattice member used in the numerical model is 2.5 mm. The AE event takes place at the micro scale, whereas the lattice element size is at the meso scale (2.5 mm) as shown in Fig.3. It is quite likely that the number of AE events at any load level will match the number of fractured lattice elements provided they are of micro size. Such a lattice simulation would demand a very large computational effort.(d) The lattice model adopted in the present study is a two dimensional model. But the cracking process is three dimensional. It should be stressed however that the trend in the cumulative number of recorded AE events with load, as shown in the Table 1 matches fairly with the trend in the cumulative number of fractured elements at the same load. AE based *b*-value analysis may be useful to investigate micro-mechanisms of fracture process in concrete. AE based *b*-value gives useful information about the various stages of the development of stress-induced cracks and fracture of concrete under bending of the samples tested.The transitions from stage V to stage VI and stage VI to stage VII can be considered as most useful for the identification of critical stage of damage as shown in Table 2 and Fig.4.

3. Conclusions

The load versus CMOD plots thus simulated agreed reasonably well with the experimental results. AE hits were recorded during the experiment and compared with the number of fractured lattice elements. It was found that the cumulative AE hits correlated well with the cumulative fractured lattice elements at all load levels thus providing a useful means for predicting when the micro-cracks form during the fracturing process, both in the pre-peak and in the post-peak regimes. A correlation between the cumulative AE hits and the cumulative fractured lattice elements at all load levels would not only provide a useful means for predicting when the micro-cracks form during the entire fracturing process, but would also increase our confidence in the lattice modeling technique. The authors opinion is that there is no direct correlation between the number of AE measurements and the number of fractured lattice elements.

Table 1: Comparison of AE hits and fractured elements in the lattice network with load

	Pre-peak zone						At Peak load	Post – peak zone					
Time (sec)	75	80	93.7	97.75	121.75	154	167	299	475	601	912	1192	1219
Load (kN)	3.88	5.27	5.56	6.192	6.06	6.74	6.79	4.63	2.51	1.88	1.0	0.478	0.45
AE hits	1197	1641	1900	2214	2365	7593	11617	29544	46844	55554	70644	77951	80951
AE events	6	10	11	12	14	50	91	331	664	803	1079	1151	1155
AE energy (volt^2-sec)	7506	9103	10447	11347	12728	47581	71008	214224	412273	512166	698360	1045492	3037577
Fractured elements	167	273	879	901	922	984	1021	1054	1136	1137	1145	1148	1151

Table 2: AE based *b*- values computed based on GBR and Aki's method for TPB specimen made with concrete

Sl.No	Feature	Phase	GBR- method			Aki's method		
			Load (kN)	Time (sec)	*b*-value*	Load (kN)	Time (sec)	*b*-value*
1	Initiation of internal cracks	I	16.5509	134	0.9039±0.0204	16.5509	134	1.647±0.0480
2	Initiation and propagation of internal cracks	II	21.338	194	1.1369±0.0185	20.8311	174	1.691±0.0481
3	Localization of cracks to form a major crack	III	22.6339	230	1.0471±0.0112	21.338	230	1.463±0.05335
4	Growth of unstable cracking	IV	20.1023	295	1.3233±0.0079	22.8051	254	1.61±0.0214
5	Micro cracks coalescence and final failure	V	15.5825	390	1.13088±0.0437	16.4188	361	1.13±0.0210

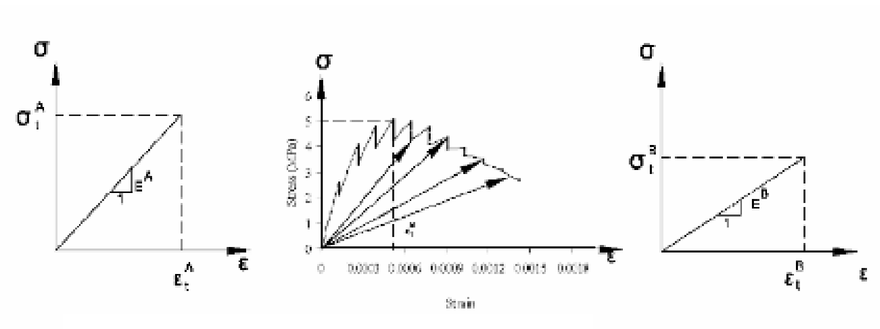

Fig.1 Material models used in the analysis

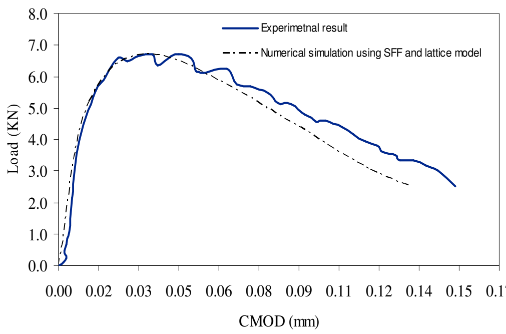

Fig.2 Comparison of experimental and numerically simulated load vs CMOD

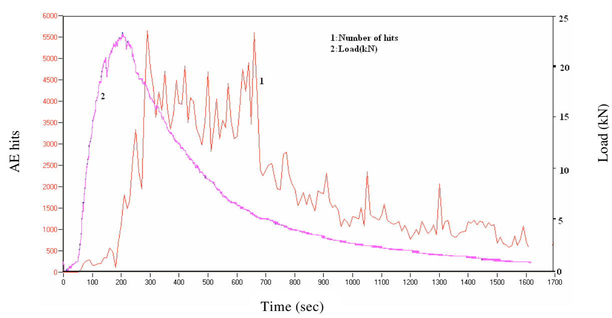

Fig.3 Typical recorded plots of load-AE as a function of time

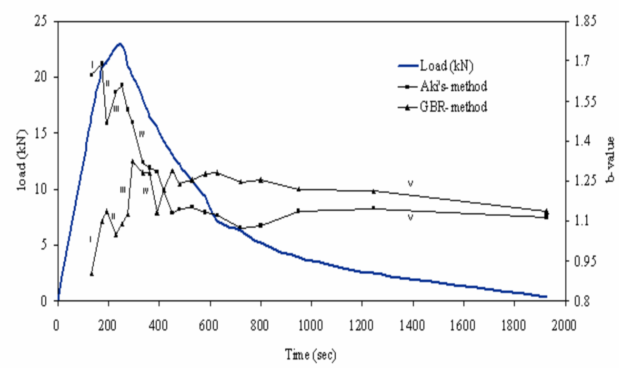

Fig.4 variation of AE based *b*-value with time

References

[1] Feder J. Fractals, Plenum, New York, 1988.

[2] Bažant Z P, Planas J,: Fracture and size effect in concrete and other quasibrittle materials, CRC Press, Boca Raton, FL 1998.

[3] Vidya Sagar R., Raghu Prasad B.K.: fracture analysis of concrete using fractal functions with lattice beam network and confirmation with acoustic emission study. *theor. Appl.Fract. Mech* **55**:192-205, 2011.

[4] Mosolov A, Singular fractal functions and mesoscopic effects in mechanics, *Cha. Sol. Fract*. **4**:2093-2102, 1994

[5] Vidya Sagar R.: Fracture Mechanics of Concrete – *Experimental and Numerical studies*. VDM-Verlag publishers; ISBN number 978-3-639-23724-5, Germany,2010.